buildings

MDPI

Article

Numerical Assessment of Different Phase Change Materials as a Passive Strategy to Reduce Energy Consumption in Buildings under Tropical Climates

Miguel Chen Austin [1,2,3], Jesús Araúz [1,4] and Dafni Mora [1,2,3,*]

[1] Research Group Energy and Comfort in Bioclimatic Buildings (ECEB), Faculty of Mechanical Engineering, Universidad Tecnológica de Panama, Panama City 0819, Panama; miguel.chen@utp.ac.pa (M.C.A.); jesus.arauz@utp.ac.pa (J.A.)
[2] Centro de Estudios Multidisciplinarios en Ciencias, Ingeniería y Tecnología (CEMCIT-AIP), Panama City 0819, Panama
[3] Sistema Nacional de Investigación (SNI), Clayton, Panama City 0816, Panama
[4] Escuela Técnica Superior de Ingenieros Industriales, Universidad Politécnica de Madrid, c/José Gutíerrez Abascal, 2, 28006 Madrid, Spain
* Correspondence: dafni.mora@utp.ac.pa

Abstract: The building envelope design constrains how much HVAC systems must work to provide comfort. High thermal mass in walls is preferable to delay heat gain, as well as reduce it. Phase Change Materials (PCMs) seem to proportionate more thermal mass without increasing wall thickness because of their high latent heat. Thus, this work studies various PCM-based envelope layouts in four case studies, H060, H100, H200, and OB, under the tropical climate of Panama City, via building energy performance simulation. Energy and thermal comfort performance were used as criteria to determine an optimal PCM-based layout for such a climate through optimization analysis and to compare PCM-based and non-PCM-based envelope layouts. Results showed that among the considered combinations, PCM-based roof configurations provide more optimum solutions than PCM-based wall configurations. The PCM layout with a melting temperature of 27 °C allowed completion of the PCM cycle throughout the year. Although other PCM layouts did not present a complete charge/discharge cycle, such as the most frequent options at H060, H100, and H200, it suggests that PCM on liquid or solid phase provides better thermal performance than other considered combinations.

Keywords: building energy performance; numerical study; phase change materials; tropical climate

Citation: Chen Austin, M.; Araúz, J.; Mora, D. Numerical Assessment of Different Phase Change Materials as a Passive Strategy to Reduce Energy Consumption in Buildings under Tropical Climates. *Buildings* **2022**, *12*, 906. https://doi.org/10.3390/buildings12070906

Academic Editor: Kee Han Kim

Received: 24 May 2022
Accepted: 21 June 2022
Published: 27 June 2022

1. Introduction

Due to the well-known climatic crisis and international agreements, such as the Paris Agreement under the United Nations Framework Convention on Climate Change, many countries are investing efforts to reduce pollution and stabilize the environment. In addition to the integration of renewable energy generation power plants [1], the role of consumers can also positively impact climate change. According to the United Nations Environment Program (2021) [2], buildings represent 36% and 37% of the final energy consumption and CO_2 emissions, respectively. Moreover, most buildings' energy consumption tends to be by heating, ventilation, and air conditioning (HVAC) systems, as in Singapore, where the Singapore Office for Energy Savings in Buildings [3] declares that more than 50% of the energy a building consumes is due to air conditioning.

Consequently, the research on building energy consumption has grown. This includes the study of thermal comfort since occupants' activities influence building energy need [4]. Furthermore, the building envelope design constrains how much HVAC systems must work to provide comfort [5]. This also applies to illumination, computers, and electrodomestics due to the relationship between user needs and energy demand. As a result, numerous

research papers analyze the optimal composition of envelope layout to determine the most appropriate combinations between the insulation and thermal mass, as in Araúz et al. [6], where novel indicators were proposed to speed up these evaluations. Commonly, high thermal mass in walls is preferable to delay heat gain and reduce it. Nevertheless, some construction restrictions exist for increasing wall mass [7].

Thus, the usage of Phase Change Materials (PCMs) seems to proportionate more thermal mass without increasing wall thickness because of their high latent heat. PCMs allow storing of a significant amount of heat, minimizing heat gains, stabilizing temperature transients during high outside temperature moments, and, consequently, achieving energy savings [8].

In this work, a review of experiments and simulations of different PCMs is carried out. The study claims to show their use in improving the thermal mass of buildings by means of passive strategies. The review methodology, PCM concept, most investigated PCMs, and PCM performance indicators are exposed. It is important to mention that the literature review is filtered to select publications related to PCM, thermal mass, and passive strategy applied mostly to tropical climates. Moreover, the review may expose the usual ways of assessing PCM-based envelopes (i.e., whether studies consider PCM and non-PCM-based envelopes within the same evaluation, interaction among PCM and non-PCM-based building elements, several types of PCMs, and within cases), which allows attending the PCM utilization problem from other perspectives. Finally, simulations of four cases of study are carried out in DesignBuilder v6.1.6.011 [9] to assess the behavior of various organic PCM types and the performance of such PCMs installed in walls and roofs in reducing the cooling energy consumption while proving various layout combinations of walls, roofs, and windows.

Therefore, this investigation aims to assess the thermal performance of different PCM-based envelope layouts compared to multiple typical roofs and wall configurations under the tropical climate of Panama City, Panama. This is to be achieved through dynamic simulations accounting for the PCMs' specific temperature-based operation ranges and changes in their thermal properties during the phase changing. In the end, it is desired that the adequate phase change material be presented for such tropical conditions (Figure 1).

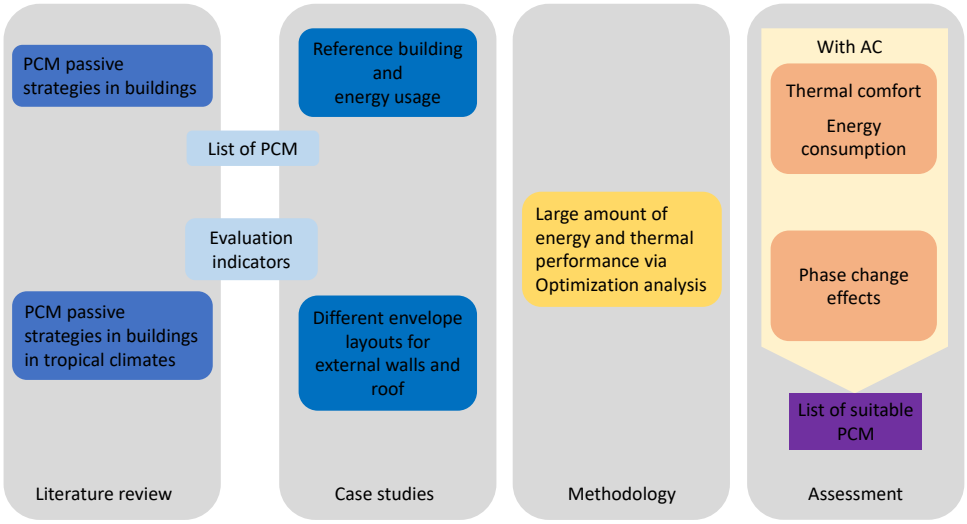

Figure 1. Research flow followed through this investigation.

1.1. PCM as Passive Strategies in Buildings

Using PCM as a construction element reduces HVAC requirements and facilitates the achievement of thermal comfort. Due to the high latent heat, PCMs have the capacity to store larger amounts of heat than common construction materials. This is because PCMs use a fraction of heat gains to change phase instead of only increasing temperature. Hence, PCMs may provide cooler temperatures than non-PCMs to the same enclosure.

There are many PCM types, but the organic ones (paraffin, fatty acids, polyethylene glycol (PEG)) are the most used. Due to their chemical stability and high latent heat, these are preferred for building applications. However, most PCMs have low thermal conductivity, which limits the optimal use of their high latent heat characteristic because of the low rate of charge/discharge [10]. Besides this, PCM can be incorporated into buildings by means of macro-encapsulated structures [11], PCM-concrete composites where block cavities are used [12], and powder-based plasters [13], among other things. However, leakages tend to appear during phase transition, and thermal conductivity decreases even more, limiting the building layout's usability. This is one of the reasons to apply PCM with support materials to overcome this restriction. Porous materials (foam, clay, graphite, silica) or nanoparticles are commonly used to stabilize PCMs structurally [14].

A considerable number of studies have been developed by means of computational simulations since these allow the assessment of multiple factors in brief periods. One of the most used softwares is EnergyPlus [15]. This is an open software made by the U.S. Department of Energy (DOE) for building energetic simulations. As an open software, it is accessible for adapting to personalized interfaces or coupling with other softwares: Sarri et al. [16] carried out a simulation-based optimization by coupling EnergyPlus and GenOpt tools to determine the optimum melting temperature of PCM when applied to buildings in different Algerian climatic zones; Jia et al. [17] used EnergyPlus to study the possibilities of improving the thermal performance of prefabricated buildings in different climates by adding PCMs; Sangwan et al. [18] also modeled a tropical building, but using Revit software to calculate cooling load, and EnergyPlus to figure out the optimal PCM thickness for energy savings. DesignBuilder [9] is also a widely used program based on EnergyPlus but with a more comfortable interface. Nematchoua et al. [19] used DesignBuilder to study the usage of passive strategy combinations, including PCM application, to reduce the cooling load and increase the comfort rate in office buildings located in different coastal tropical climates; Bimaganbetova et al. [20] performed numerical simulations in DesignBuilder to investigate the thermal behavior of residential buildings with tropical savanna climate, where eleven PCMs were considered as well as their location in the building layout; Berrocal et al. [21] developed numerical studies by means of DesignBuilder to assess the thermal behavior of tropical buildings by comparing their performance with many PCM-based and non-PCM-based envelopes.

On the other hand, although computational simulations provide faster results than experimental procedures, some recent works developed experimental studies to assess real PCM in tropical climates: Saxena et al. [22] measured the temperature reduction on a building improved with PCM-embedded bricks with one and two layers; Rathore and Shukla [8] evaluated the thermal response of a building under a real tropical climate by means of erecting two concrete-based cubicles, where only one had aluminum-based macrocapsules of PCM; Hakim et al. [12] also compared inner wall temperature between a case with PCM added to brick cavities and a case with only concrete bricks; Cardenas-Ramírez et al. [13] calculated the thermal transmittance, heat storage capacity, and thermal inertia of different combinations of three shape-stabilize PCMs experimentally.

1.2. Performance Evaluation of PCMs and Criteria

Considering the wide variety of PCMs, a way of comparing each one's performance is needed. Besides the inherent characteristics of each PCM, according to their chemical composition, their usage in a building also influences the achievable benefits. Furthermore, research works tend to establish a comparison framework where PCM behavior is analyzed. Due to PCMs' characteristics, it is possible to compare them with insulation materials as well as thermal masses. Yu et al. [23] studied a roof with outer-layer shape-stabilized PCM, where its heat insulation properties were assessed by the time lag, decrement factor, liquefaction rate, and utilization rate of latent heat. Moreover, the phase transition temperature, phase transition temperature radius, and PCM layer thickness were considered. Bhamare et al. [24] developed a full tridimensional model in ANSYS to assess the thermal

performance of a residential building roof with an inclined PCM layer. The ceiling temperature, peak heat load reduction, daily heat gains, decremental factor, and melting and solidification cycle were evaluated as functions of the PCM layer inclination and concrete mass. Other authors, such as Imghoure et al. [25], compared PCMs by analytic hierarchy processes, where common performance indicators, such as time lag and decremental factor, are evaluated by comparing PCM characteristics. Some of these are phase change temperature, density during solid phase, latent heat capacity, thermal conductivity during liquid and solid phases, and specific heat capacity.

As mentioned, there are multiple variables to analyze the benefits of installing PCMs in buildings. By reviewing some recent works, it can be concluded that the PCM performance can be evaluated by examining the thermal behavior of buildings and the PCM layer. A classification based on both systems' thermal responses, building, and PCM, is selected to assess PCM as a passive strategy to reduce energy consumption and decrease thermal discomfort hours. Thus, indoor temperature, envelope heat gains, discomfort hours, indoor temperature, and building net energy consumption, among other things, could be some of the building evaluation parameters to assess PCM performance, as latent heat utilization, phase transition temperature, phase changing cycle, etc., can be used as PCM parameters to evaluate PCM performance.

In addition, the coupling between PCM as a passive strategy and other techniques is frequently analyzed. Therefore, the combination of shading devices, natural ventilation, insulation layers, reflective surfaces, thermal mass layers, etc., is considered. The following subsections contain the results and remarkable annotations of the reviewed research articles—several articles provided conclusions in more than one performance criterion.

1.2.1. Indoor Temperature

Imghoure et al. [25] declared temperatures around 23.5 °C, where maximum temperature without PCM implementation exceeds 30 °C. Moreover, the decrement factor was decreased from 0.2 to almost 0.0014, and the thermal lag was increased from 4 h to 7 h. Bhamare et al. [24] achieved ceiling temperature ranges between 25.5 °C and 27.5 °C by adding inclined PCM layer. This represents an improved time lag range between 6 h and 7 h and a decrement factor range between 0.043 and 0.082 when the non-PCM roof provides 5 h and 0.155, respectively. Yu et al. [23] considered the modeling of PCMs with different phase transition temperatures. PCM implementation offered an inner roof temperature range between 29 °C and 33 °C, when, without PCM, it varied between 28 °C and 35 °C. This represents a decrement factor improvement from 0.232 to 0.14–0.033 and an increase of time lag from 5 h to 7–8 h. Saxena et al. [22] tested PCM-embedded bricks, where reductions of 9.5 °C and 6 °C were achieved with a single PCM layer and a double PCM layer, respectively. Cárdenas-Ramírez et al. [13] exposed, by an experimental setup, how using stabilized-shape PCM-based acrylic plaster increases thermal lag by 67.26%, decreases by 9% the decrement factor, and provides an indoor temperature reduction of 20.8%. Moreover, the usage of PCMs as powder can increase the thermal lag by between 148% to 180% depending on the PCM type. Rathore and Shukla [11] achieved a reduction of 53.19% in the thermal amplitude (1-DTPCM/DTref) inside ambient and reductions of surface temperatures ranging from 40.67% to 59.79%. These reduction scenarios correspond to reductions in peak temperature from 7.36% to 9.18%. Bimaganbetova et al. [18] simulated a two-floor residential in eight different tropical climates. Applying the PCM layer can reduce peak temperatures up to 3.28 °C. Moreover, temperature fluctuations are reduced from a range between 5.51 °C and 7.34°C to a range between 2.30 °C and 4.37 °C. This represents that PCM can reduce peaks and fluctuations in buildings.

1.2.2. PCM Layer Location

Imghoure et al. [25] considered six configurations made up with layers of mortar, brick, insulator, and PCM. The results show that placing PCM close to the hottest surface and after an insulation layer provides more utilization of the PCM layer since it absorbs more

heat. Thus, better thermal performance is obtained. Bhamare et al. [24] did not consider changing the PCM layer location. However, they did consider inclination angles from 0° to 4°, where the 2° case presented the highest time lag and the lowest decrement factor. Jia et al. [17] simulated a prefabricated building in five different locations to assess the influence of PCM on walls and roofs. According to the results, placing PCM on the inner wall surface is better than on the outer one, as well as in roofs, where greater savings are obtained when installing PCMs on the inner roof surface.

Furthermore, regardless of the climate zone, the best place for adding PCMs, according to the energy savings per unit PCM area, is the east and west wall sides, followed by roofs and north and south wall sides. However, focusing on global energy savings, installing PCM on roofs mainly and on all wall surfaces would provide the greatest energy savings, but focusing on cost performance, PCMs should only be installed on east and west wall sides. Bimaganbetova et al. [20] concluded that the internal layers of PCMs, as the external ones, provide very similar energy savings. However, among the four considered locations, external PCM layers tend to provide better energy savings at higher thicknesses, in contrast to internal layers, which seem to provide more energy savings at smaller thicknesses. Sangwan et al. [18] also showed that PCM external-wall side layers provide a lower cooling load. However, the results showed that internal wall-side PCM layers establish a slight extra energy consumption reduction in walls compared to external ones, although external ones provide the lowest net energy consumption. It is observed that PCM layer location has little influence on energy consumption.

1.2.3. Phase Changing Operation

Imghoure et al. [25] considered five different PCMs as alternatives for buildings. It was found that those PCMs with melting temperatures near the average daily temperature provide more comfort since the liquid phase is more frequent than other PCMs with higher melting temperatures. Bhamare et al. [24] analyzed the influence of PCM layer inclination on the melting and solidification cycle, and it was observed that the configuration which provided better thermal performance (2 °C) achieved a 39% melting and solidification cycle, when the other considered configurations achieved 32% and 22%. Thus, the charging/discharging capacity usage was better in the 2° case. Bhamare et al. [24] also used the average Nusselt number to qualify the storage and release of heat, and the performance of the 2° case showed more heat storage than the others. Yu et al. [23] concluded that phase transition temperature has little effect on the average room temperature; however, it does have considerable influence on peak temperature, thus, on the decrement factor. Yu et al. [23] also showed how the liquefaction rate varied from 76% to 96% according to an increment of 2 °C on phase transition temperature. Sarri et al. [16] determined the optimum melting temperature for PCM in a building studied in different Algerian climates. A temperature of 28 °C, with a melting range of 3 °C, is obtained to ensure a comfort range of 24 °C to 27 °C, where outdoor air temperatures are up to 48 °C. Moreover, it is remarkable that coupling shading devices to PCM decreased melting temperature need to 27.07 °C. Jia et al. [17] showed how the latent heat and the phase transition temperature are related to energy savings. By comparing the thermal performance of a reference building in different climates, it was found that more latent heat provides more savings no matter the climate zone. Moreover, a near-average PCM transition temperature is preferred for increasing energy savings.

1.2.4. PCM Layer Thickness

Imghoure et al. [25] did not vary the thickness of the PCM layer but remarked that adjusting the thickness can be a solution for a specific phase transition period. In Yu et al.'s [23] simulations, it was found that thickness beyond 30 mm does not improve thermal behavior (temperature range and liquefaction rate). Hence, an optimal thickness of 30 mm is preferred among other configurations. Yu et al. [23] also showed how the fluctuations of liquefaction rate are reduced by increasing PCM layer thickness (from 5 mm to 30 mm).

Saxena et al. [22] remarked that increasing PCM layer thickness could provide better peak temperature reduction as long as the heat discharging during the night is ensured by any auxiliary process since a higher thickness would make night discharging difficult. Jia et al. [17] studied the relation of PCM layer thickness to energy savings by means of simulations that considered five different climates. According to the results, increasing the thickness increases energy savings and thermal comfort, but the rate reduces rapidly while the PCM cost increases linearly. Thus, a minimum thickness of 10 mm is suggested as the most cost-effective solution. Bimaganbetova et al. [20] showed by simulation that the rate of energy consumption reduction achieved by increasing thickness decreases at higher thicknesses. For example, a thickness of 5 mm provided around 6% energy consumption reduction per millimeter, but a thickness of 40 mm provided 2%. On the other hand, in a constant volume scenario, the smallest thickness and largest areas provided higher annual energy savings.

1.2.5. PCM Coupled to Other Passive Techniques

Imghoure et al. [25] proved the influence of insulator layers on PCM thermal behavior by changing their relative positions in the wall envelope. The results indicated that using an insulator before the PCM layer allows PCM to reduce its transformation rate since the insulator reduces heat gains. Saxena et al. [22] proved different PCM encapsulation, and it was seen that using metal fins in metal casing adversely affects PCM thermal behavior. This is because fins increase the heat rate; thus, the temperature rises higher than admissible to allow an appropriate night discharge. Cárdenas-Ramírez et al. [13] tested stabilized shape-PCM-based acrylic plaster used as fiber cement siding finish in combination with insulating paint. It was found that combining both techniques provided a smaller decrement factor, larger thermal lag, and smaller thermal transmittance than using only insulating paint. The combination provided 3.38 times more thermal lag, a 2% reduction of decrement factor, and a 32% reduction of thermal transmittance. Nematchoua et al. [19] simulated a building in four different climates with insulation, insulation and shading, and insulation and PCM. The comfort rate without passive techniques ranges from 65% to 80.3%, with insulation from 65.1% to 80.8%, insulation and shading from 65.2% to 81.4%, and insulation and PCM from 65.5% to 82.2%. On the other hand, different energy savings were achieved: with insulation from 8.88% to 10.21%, with local shading from 2.45% to 5.05%, insulation and shading from 18.79% to 20.06%, and with insulation and PCM from 11.87% to 12.44%. Moreover, the results showed that combining PCM with insulation provides a temperature stabilization band from 23 °C to 26 °C. In contrast, the outside temperature is under 19 °C and over 28 °C. Sarri et al. [16] assessed the effect of using PCMs and shading devices in different hot Algerian locations. It was found that adding shading devices to buildings with PCM can improve energy savings up to 33.83%, compared to a buildings thermally improved with PCM.

1.2.6. Energy Consumption and Cooling Load Reduction

Bhamare et al. [24] concluded that the best inclination for heat gain reduction of a PCM layer into a slab is 2°. A comparison between a non-PCM slab, and inclined PCM layers (0°, 2°, 4°) showed maximum heat gains of 49 W/m^2, 38.43 W/m^2, 29.22 W/m^2, and 36.27 W/m^2, respectively. Moreover, following the same order, daily heat gains of 636 Wh/m^2, 654 Wh/m^2, 604 Wh/m^2, and 0.530 Wh/m^2 were found. Saxena et al. [22] achieved heat gain reductions up to 40% and 60% for single and double PCM layers, respectively. However, this performance is worse during the night. Then, the overall heat reduction ranges from 16% to 20%. Rathore and Shukla [11] compared the benefits of macrocapsules of PCM in buildings by constructing two identical cubicles (length = 1.12 m). The cubicle with PCM provided a reduction from 19.41% to 41.31% of peak heat flux depending on wall orientation. Moreover, a cooling load reduction of 38.76% was achieved, representing a cost saving of USD 0.4/day. Sarri et al. [16] simulated a building in different Algerian climates through four seasons, and it was found that installing PCM provided

energy savings from 3.37% to 6.87% in summer. Moreover, the usage of PCM reduced cooling energy consumption by 7.12% and up to 31.22%. Bimaganbetova et al. [20] proved 29 PCM options for improving building thermal performance across eight different tropical locations. Results showed energy consumption reductions from 14.66% to 68.63%, according to the outdoor temperature profile.

1.2.7. Heating and Cooling Demand Depending on the Climate Type

From the simulation developed by Arce et al. [26], where an enclosure without PCM and another with PCM are compared, it is observed that the demand for cooling decreases when PCM is used in all the localities studied (Antarctica, Latvia, Lebanon, Mali, and Turkey). Jahangir et al. [17] compared the energy behavior of a P56-58 paraffin wax PCM against brick, sand, and air and found that both PCM and brick had better energy behavior than sand and air. This shows that its implementation is more appropriate for reducing temperature variations. The general heat flow exhibits a trend similar to that reported by Hasan et al. [27], who determined that integrating a PCM layer reduces the maximum heat flux.

On the other hand, Li et al. [19] studied the behavior of a brick wall compared to a brick wall with a PCM layer. In this investigation, it was found that the temperature of the interior surface of the wall with the PCM is lower than the temperature of the inside surface of the reference wall. Similarly, it was found that the heat flux in the PCM wall is less than the reference wall.

2. Methodology

Performing the literature review has allowed us to identify the most common phase change materials used in building applications for passive strategies. To evaluate the implementation of such materials in a tropical climate as in Panama City, five phase change materials were chosen for performing a numerical study. For this evaluation, optimization analyses were performed through the EnergyPlus-based interface DesignBuilder v6.1.6.011.

DesignBuilder software is an interface high-quality, easy-to-use simulation software that allows for quickly assessment of the environmental performance of buildings. It is an advanced building performance simulation tool that minimizes modeling time and maximizes productivity. Imported or built-in DesignBuilder models provide fully integrated performance analysis, including energy and comfort, cost, HVAC, design optimization, daylighting, BREEAM/LEED credits, CFD, and reports complying with several building regulations and certification standards [9].

2.1. Buildings Descriptions and Energy Use

Four different building typologies were selected for this study, as shown in Figure 2. Three one-storey buildings with a floor area of 60 m^2 (Figure 2a), 100 m^2 (Figure 2b), and 375 m^2 (office building), named H060, H100, and OB, respectively. Moreover, a house with 200 m^2 floor area, named H200. Such buildings represent the most common standard residence floor areas in Panama City. No windows were considered on the posterior side for the H060, H100, and H200, as is customary in most cases.

The physical characteristics of each building envelope are described in Table 1, along with the building orientation, and occupancy density chosen for this study. For the external walls (original walls), a 0.01 m mortar layer was followed by a 0.1 m heavyweight concrete layer and a 0.01 m mortar layer. For the internal partitions, there was a 0.01 m mortar-cellular-cement layer followed by a 0.1 m heavyweight concrete layer and a 0.01 m mortar-cellular-cement layer. Both layouts were chosen based on the local standard construction tendency. For the floor, there was a 0.1 m cast dense concrete as external layer and a 0.016 m granite as the internal layer. The roof in H060, H100, and H200 was composed of zinc layers followed by a 0.5 m air gap. On the contrary, for the OB, the roof was a 0.2 m concrete-based slab followed by a 0.5 m air gap and a 0.02 m gypsum-plasterboard layer. Finally, clear

single-layer windows were chosen for the H060, H100, H200, and solar-grey double-layer windows for the OB.

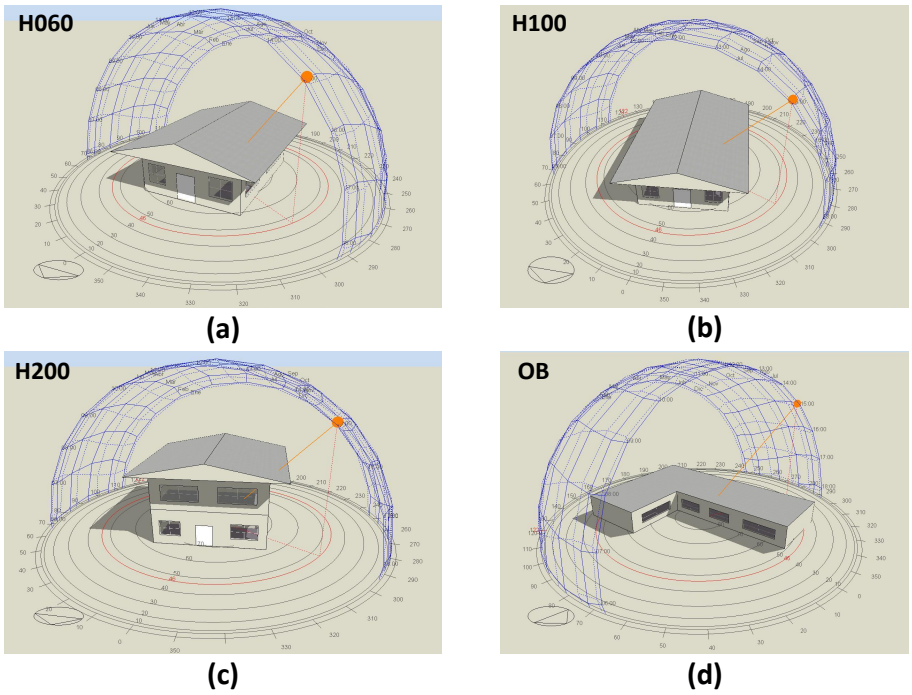

Figure 2. Four different dwellings tested: (**a**) 60 m^2, (**b**) 100 m^2, (**c**) 200 m^2, and (**d**) 375 m^2 office building.

Table 1. Summary of the U-values for each envelope element in the reference buildings.

Building	Floor Area (m^2)	WWR (%)	Orientation (°)	U-Value (W/m^2K)					Occupancy Density (p/m^2)
				External Walls	Internal Partitions	Floor	Roof	Windows	
H060	60	30	180	3.859	2.618	3.487	7.071	5.778	0.111
H100	100								
H200	200								
OB	375						1.486	1.96	0.05

Moreover, both repeating and non-repeating material thermal bridges were not considered. Good air tightness along with a calculation-based ventilation were chosen (Table 2). Calculation-based ventilation refers to the way of determining the air change rate (ach) and airflow within the building zones and exterior, based on the available wind speed and direction at each opening, and the indoor–outdoor temperature difference. This option can be selected in the software for more accurate results, contrary to the default schedule-based ventilation with a constant ach value. Moreover, internal gains and schedules, such as for household equipment, occupancy, and lightning, were considered as shown in Table 2.

All simulations were performed under the tropical climate of Panama City gathered in a typical meteorological data file obtained from CLIMdata Solargis® (Table 3). The outdoor air dry-bulb temperature ranges from 20.6 to 35.6 °C.

Table 2. Different energy usage profiles in the reference buildings.

Energy Usage	Profiles		Value
	Houses	Office Building	
Occupancy	8:00–19:00		Density
Natural ventilation	20:00–7:00		Calculated
Infiltration (ach/h)	24/7		0.7
Lightning (W/m^2-100 lux)	19:00–0:00		3.3
Air conditioning (Splits)	8:00–19:00		COP = 3.0
Household equipment (W/m^2)	24/7		11.77

Table 3. Typical meteorological data used for simulations.

Month Critical Day	T_{max} (°C) Hour	T_{min} (°C) Hour	HR_{max} (%) Hour	HR_{min} (%) Hour	Wind Speed (m/s)	Wind Direction (°)
3 January	35 15:00	23.9 6:00	94 5:00	44 15:00	0.43	126
20 February	34.6 15:00	22.2 6:00	93 6:00	40 15:00	2.77	85.77
17 March	35.6 15:00	24.9 6:00	73 6:00	36 16:00	2.3	49
11 April	35.3 15:00	24.8 6:00	82 24:00	44 16:00	1.75	87
20 May	34.8 15:00	24.5 6:00	90 6:00	53 16:00	0.87	83.3
23 June	32.8 15:00	23.4 6:00	94 6:00	58 15:00	0.45	108.25
21 July	35.5 16:00	24.3 6:00	97 4:00	49 16:00	0.3	89.3
19 August	34.7 15:00	24.1 6:00	95 5:00	52 15:00	3.9	188
1 September	32.5 15:00	23 6:00	98 24:00	60 15:00	2.1	83
20 October	32.5 15:00	23 6:00	96 6:00	62 14:00	2.33	90.67
11 November	32.9 15:00	23.7 6:00	94 5:00	61 13:00	2.55	80
16 December	34.3 15:00	24.6 6:00	94 7:00	50 16:00	4.2	34.5

2.2. Evaluation of Different Building Envelope Layouts

For the evaluation of different building envelope layouts, several roof layouts, external-wall layouts, and glazing types were implemented as shown in Table 4. The roof and external-wall layouts were chosen to contain different thermal mass and insulation degrees available in the local market. The evaluation of each envelope layout was performed to look for the combinations of roof+wall+glazing that allow minimizing both the discomfort hours (DH) and the energy consumption for cooling (EC) via optimization analysis. Minimizing electricity consumption for cooling and occupants' discomfort hours were the objectives stipulated for the optimization analysis. The adaptive comfort with 80% acceptability based on the ASHRAE 55 standard was chosen for the thermal comfort. No constraints were considered for the optimization objectives. The monthly averaged simulation results from the whole year were used in the optimization analysis. The parameters chosen as design variables are presented in Table 4. In addition, the window-to-wall ratio (WWR) and the building orientation were also included in the optimization analysis. There were no restrictions other than a range between 30% to 50% for the WWR. Among the roof and external-wall layouts, five PCM-based layouts were included.

The method used in the optimization analysis is based on the genetic algorithms (GAs). A GA allows identifying the adequate configurations, applying an iterative generational analysis process, including the following steps: encoding variables and design options, random generation of an initial population, file generation, simulation in EnergyPlus of the first solutions and analysis of results, classification of solutions, selection of "parents" (tournament), crossover and mutation, EnergyPlus simulation, the union of parents and offspring, repetition of the process, the established number of iterations, and finally the analysis of the best solutions shown on the Pareto front [28]. The settings applied were: maximum generations of 100, generation for convergence of 5, an initial population of 20, optimization Engine JEA [29], generation population size of 20, maximum population size of 10,000, and mutation rate of 0.40.

The evaluation of phase change materials (PCMs) as part of the envelope was performed by introducing the most common PCM used for passive building applications mentioned before. Different PCM-based layouts were implemented based on the standard PCM-based roof and walls considered in DesignBuilder, which also includes further aspects such as the encapsulation of the PCM (Figure 3). The EC for all best combinations characterized by laying within the Pareto's front was also compared with each reference building EC for cooling.

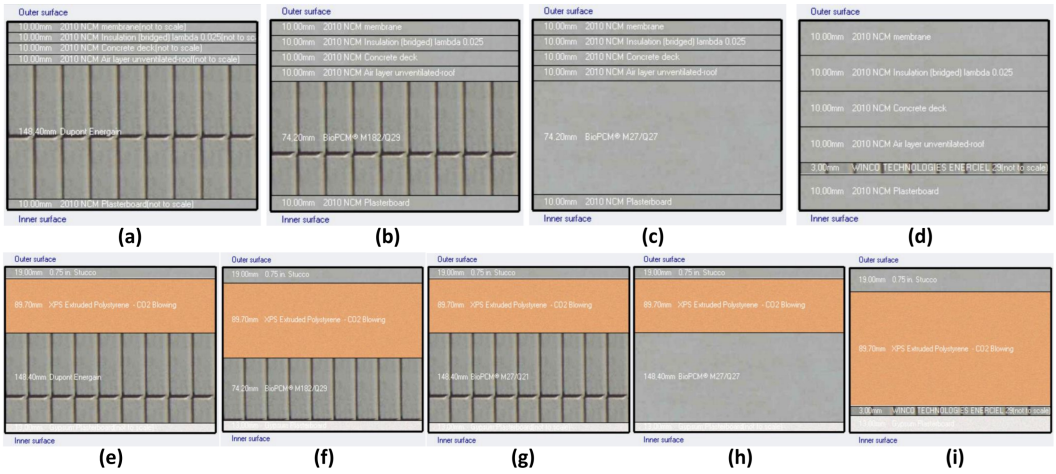

Figure 3. Five different standard PCM-based layouts tested [9]. For the roof layout: (**a**) Q25 Dupont Energain, (**b**) M182/Q29, (**c**) $m^2$7/Q27, and (**d**) Winco Q29. For external-wall layout: (**e**) Q25 Dupont Energain, (**f**) M182/Q29, (**g**) $m^2$7/Q21, (**h**) $m^2$7/Q27, and (**i**) Winco Q29.

For the roof layout, the standard PCM-based layout contains (from external to internal) a 0.01 m NCM membrane, 0.01 m of insulation, 0.01 m concrete, 0.01 air layer, followed by the PCM layer whose thickness varies depending on the PCM type, and finally, a 0.01 m plasterboard layer (Figure 3a–d). In contrast, for the layout of the external walls, the standard PCM-based layout contains (from external to internal) a 0.019 m of Stucco, 0.0897 m XPS EP, followed by the PCM layer, whose thickness also differs depending on the PCM type, followed by a 0.013 m Gypsum plasterboard layer (Figure 3e–i).

Moreover, optimization analyses were also performed considering the PCM-based layouts in Figure 3, but with their layers were inverted, along with the other non-PCM-based layouts presented in Table 4, with the intention of assessing different positions of the PCM layer within the layout. Finally, since some PCM-based layouts present very low U-values similar to other non-PCM-based layouts tested, any resulting layout containing a PCM layer was further analyzed in terms of roof and wall surface temperatures and the corresponding PCM melting temperature point (MTP). This was done in order to discern whether such a resulting PCM-based layout was chosen over a non-PCM-based layout because of the phase change behavior or only for their very low U-values.

Table 4. Summary of the envelope layouts tested.

Component	Proposed Options as in DB	e (m)	U (W/m^2-K)	Justification	Nomenclature
Roof	Original roof	0.005	7.143	Reference building	RRB
	25 mm Stone Chippings, 19 mm Asphalt, 40 mm Roof Screed	0.084	3.439	Available layout in local market	Rop1
	19 mm Asphalt, on 13 mm fiberboard on 25 mm eps slab	0.057	0.991		Rop2
	Flat roof 0.25	0.154	0.252		Rop3
	Pitched roof Energy code standard—Heavyweight	0.212	0.211		Rop4
	State-of-the-art—Heavyweight	0.18	0.486		Rop5
	0.5 metal zinc, 75 mm EPS (Not in DB)	0.076	0.496		Rop6
	Superinsulated	0.364	0.258		Rop7
	Pitched roof Uninsulated Medium weight	0.05	2.93		Rop8
	200 mm concrete slab + air + gypsum	0.72	1.486		Rop9
	Clay tiles (25 mm) on airgap (20 mm) on roofing felt 5 mm	0.05	2.93		Rop10
	Uninsulated heavyweight	0.132	1.546		Rop11
	BioPCM M27Q25 Roof Dupont Energain	0.198	0.113	From literature	Rop12
	BioPCM Roof M182/Q29	0.124	0.991		Rop13
	BioPCM Roof M27/Q27	0.124	0.991		Rop14
	WincoPCM Roof 29	0.053	1.519		Rop15
	PCM-based roof layouts in inverse position	–	–		Rop16–Rop19
Walls	Original walls	0.120	3.859	Reference building	WRB
	State-of-the-art—Heavyweight	0.293	0.350	Available layout in local market	Wop1
	Super insulated brick/block	0.425	0.156		Wop2
	Lightweight superinsulated	0.102	0.375		Wop3
	Energy code standard—Heavyweight in DB	0.263	0.500		Wop4
	Uninsulated medium weight	0.213	2.071		Wop5
	Brick air m/w concrete block & phenolic foam & l/w plas	0.268	0.825		Wop6
	Brick air uf insulation l/w concrete block & l/w plaster	0.268	0.596		Wop7
	Lightweight concrete block air gap & plasterboard	0.236	0.708		Wop8
	Brick cavity with dense plaster	0.268	1.562		Wop9
	Brick air l/w concrete block & l/w plaster	0.273	1.562		Wop10
	BioPCM Wall Dupont Energain	0.27	0.09	From literature	Wop11
	BioPCM Wall M182/Q29	0.196	0.308		Wop12
	BioPCM Wall M27/Q27	0.270	0.277		Wop13
	WincoPCM Wall 29	0.125	0.345		Wop14
	BioPCM Wall M27/Q21	0.270	0.277		Wop15
	PCM-based wall layouts in inverse position	–	–		Wop16 –Wop19

Table 4. *Cont.*

Component	Proposed Options as in DB	e (m)	U (W/m^2-K)	Justification	Nomenclature
Windows (glazing)	Original windows (Sgl Clr 6 mm as in DB)		6.121	Reference building	GRB
	Dbl Clr 4 mm/16 mm Air		2.715		Gop2
	Dbl Clr 6 mm/12 mm Air		2.685		Gop3
	Sgl Bronze 6 mm		6.121		Gop6
	Dbl Solar Grey 6 mm/12 mm Air		3.157		Gop7
	Dbl Clr 4 mm/12 mm Air		2.725		Gop8

3. Results Analysis

3.1. Performance of Different Envelope Layouts Tested

The results from optimization analysis for each of the buildings studied (Figure 2) are presented in Figures 4–7. Here, only the optimized cases at Pareto's front are presented, where colors were used to identify the roof layouts and the marker shapes serve to identify the external-wall layouts. The colored regions in the plots give indications of the dominant color, i.e., the dominant or preferable roof layouts. From Figures 5–7, a clear dominant roof layout can be observed. However, the most present or most frequent solution is chosen to be examined instead of analyzing the solutions at minimum electricity consumption (EC) or minimum discomfort hours (DH). This is done before identifying the adequate option based on the best EC and DH compromise with a less subjective assessment. For this purpose, Tables 5–8 show the resulting count of each layout combination for H060, H100, H200, and OB, respectively.

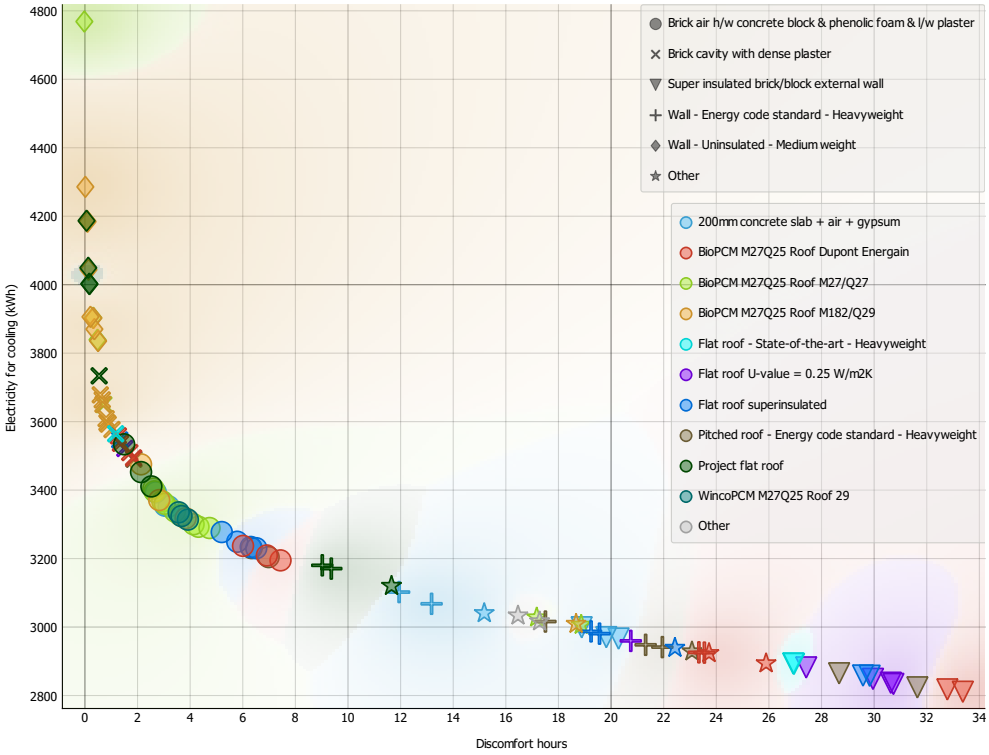

Figure 4. Optimization analysis result at Pareto's front for the H060 operating in AC mode.

Table 5. Resulting counts of each layout combination that appeared at Pareto's front for the 60 m^2 building.

Roof Construction	External Wall Construction						Total
	Wop6	Wop10	Wop2	Wop4	Wop1	Wop5	
Rop9	3	0	3	2	1	0	9
Rop12	3	4	2	2	2	0	13
Rop14	9	1	0	0	2	3	15
Rop13	3	7	0	0	1	8	19
Rop5	0	1	2	0	0	0	3
Rop3	0	1	4	1	0	0	6
Rop7	4	1	2	2	1	0	10
Rop4	2	1	2	3	1	0	9
RRB	3	1	0	2	3	4	13
Rop15	3	0	0	0	0	0	3
Total	30	17	15	12	11	15	100

For the H060 (Table 5), 100 solutions appeared at Pareto's front, where the most that appeared concerning the roof and external-wall layouts were Rop13 and Wop6, respectively. The Rop13 layout is PCM-based (Table 4). In this case, the combination Rop13 with Wop6 is associated with a Gop4, an orientation of 250°, and 30% WWR. For the H100 (Table 6), 98 solutions appeared at Pareto's front, where the most that appeared concerning the roof and external-wall layouts were RRB and Wop6, respectively. Neither of these layouts is a PCM-based layout (Table 4). For the H200 (Table 7), 74 solutions appeared at Pareto's front, where the most that appeared concerning the roof and external-wall layouts were Rop12 and Wop5, respectively. The Rop12 layout is PCM-based (Table 4). In this case, the combination Rop12 with Wop5 is associated with a Gop4, an orientation of 220°, and 30% WWR. Finally, for the OB (Table 8), 58 solutions appeared at Pareto's front, where the most that appeared concerning the roof and external-wall layouts were Rop14 and Wop15, respectively. Both layouts are PCM-based layouts (Table 4). In this case, the combination Rop14 with Wop15 is associated with a Gop4, an orientation of 325°, and 30% WWR.

Furthermore, the position of the PCM layer within each PCM-based layout was also assessed by inverting the original positions of their layers. The PCM layer gets closer to the external surface by inverting its layers. However, the optimization analysis results indicated that such an inverted-PCM-based layout configuration is neither preferred nor offers more benefits than the other non-PCM-based layouts tested since such inverted-PCM-based layouts did not fall in Pareto's front.

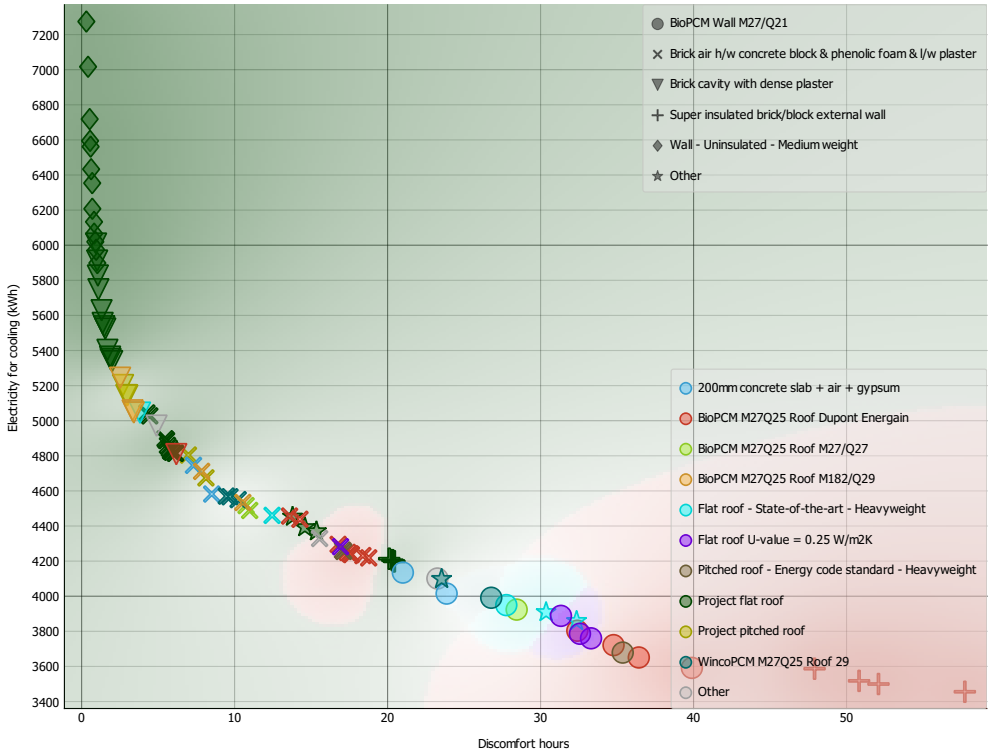

Figure 5. Optimization analysis result at Pareto's front for the H100 operating in AC mode.

Table 6. Resulting counts of each layout combination that appeared at Pareto's front for the 100 m^2 building.

Roof Construction	External Wall Construction							Total
	Wop15	Wop6	Wop10	Wop2	Wop4	Wop1	Wop5	
Rop9	2	2	0	0	0	0	0	4
Rop12	4	8	1	4	0	0	0	17
Rop14	1	2	0	0	0	0	0	3
Rop13	0	2	3	0	0	0	0	5
Rop1	1	0	0	0	0	0	0	1
Rop5	1	1	1	0	1	1	0	5
Rop3	3	1	0	0	0	0	0	4
Rop7	0	1	1	0	0	0	0	2
Rop4	1	2	0	0	0	0	0	3
RRB	0	14	15	4	3	0	13	49
Rop15	1	3	0	0	1	0	0	5
Total	14	36	21	8	5	1	13	98

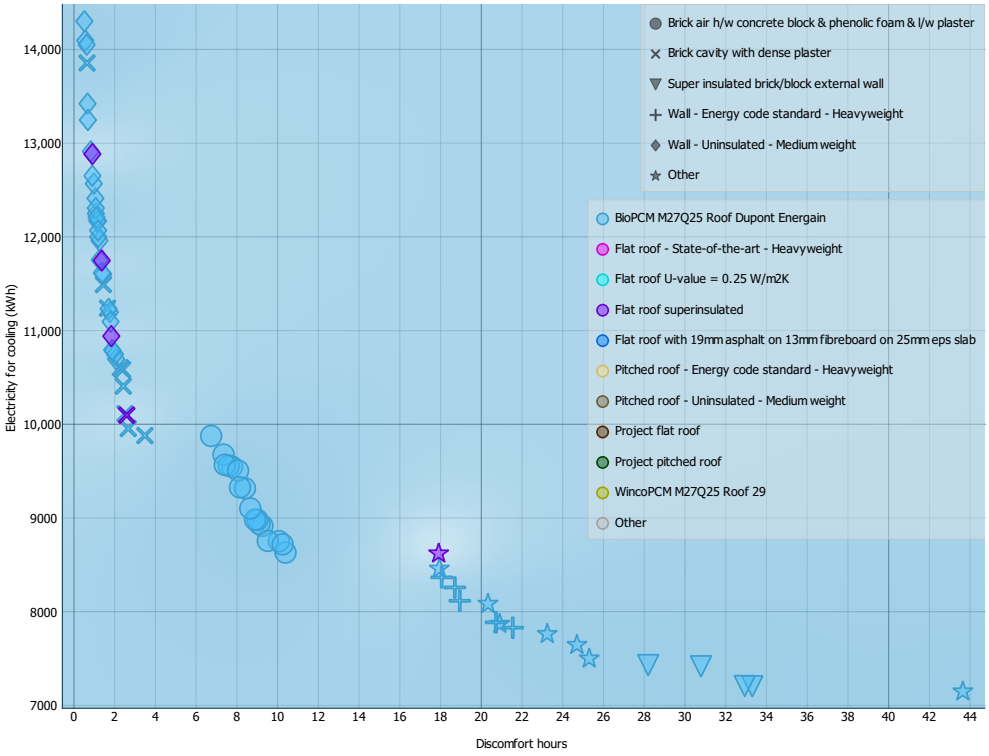

Figure 6. Optimization analysis result at Pareto's front for the H200 operating in AC mode.

Table 7. Resulting counts of each layout combination that appeared at Pareto's front for the 200 m^2 building.

Roof Construction	External Wall Construction									Total
	Wop11	Wop15	Wop6	Wop7	Wop9	Wop2	Wop4	Wop1	Wop5	
Rop12	1	3	17	1	9	4	5	2	27	69
Rop7	0	1	0	0	1	0	0	0	3	5
Total	1	4	17	1	10	4	5	2	30	74

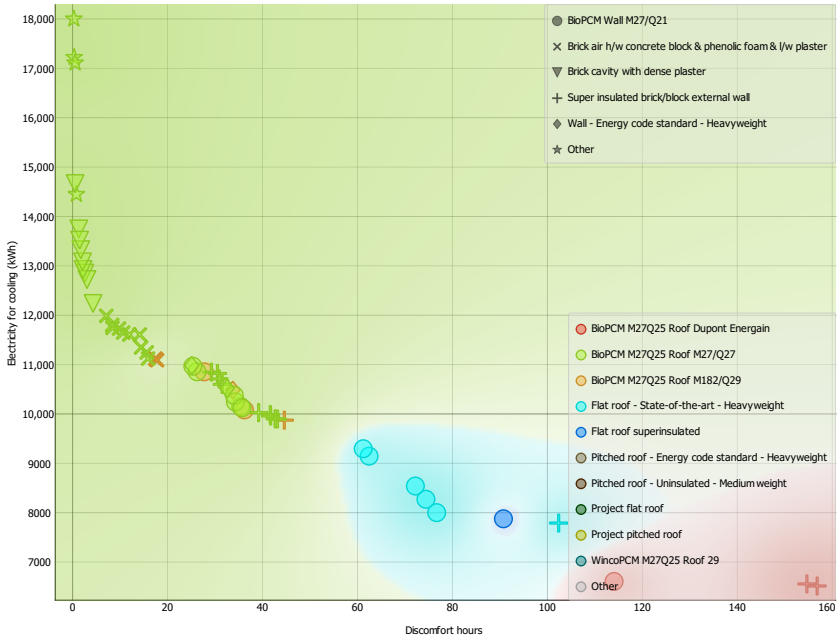

Figure 7. Optimization analysis result at Pareto's front for the OB operating in AC mode.

Table 8. Resulting counts of each layout combination that appeared at Pareto's front for the Office Building.

Roof Construction	External Wall Construction							Total
	Wop15	Wop6	Wop9	WRB	Wop2	Wop4	Wop5	
Rop12	1	0	0	0	2	0	0	3
Rop14	6	10	9	3	9	3	1	41
Rop13	2	3	0	0	1	1	0	7
Rop5	5	0	0	0	1	0	0	6
Rop7	1	0	0	0	0	0	0	1
Total	15	13	9	3	13	4	1	58

3.2. Energy Consumption for Cooling and Envelope Layouts

The previous results and analysis have shown a clear and significant tendency or preference to choose PCM-based layouts (roof and external-wall constructions) over non-PCM layouts at Pareto's front. In fact, by comparing each EC of solutions at Pareto's front to the corresponding reference building EC, Figures 8–11 show that, for each building, the highest EC reduction for cooling (>50%) is achieved when a PCM-based layout is considered as part of the roof construction, with the Dupont Energain BioPCM being the layout showing the highest reduction in all four cases. In contrast, to achieve the lowest DH (corresponding to the minimum EC reduction), only for the H060 (Figure 8), H200 (Figure 10), and the OB (Figure 11) a roof PCM-based layout is preferred. On the other hand, a weak insulation degree layout for external walls is preferred for each building. Finally, from Figures 8–11, the best compromise between the lowest possible DH and the highest possible EC for cooling appeared to be found when choosing a brick air phenolic layout for external walls (Wop6) for each building, and a PCM-based layout for the roof.

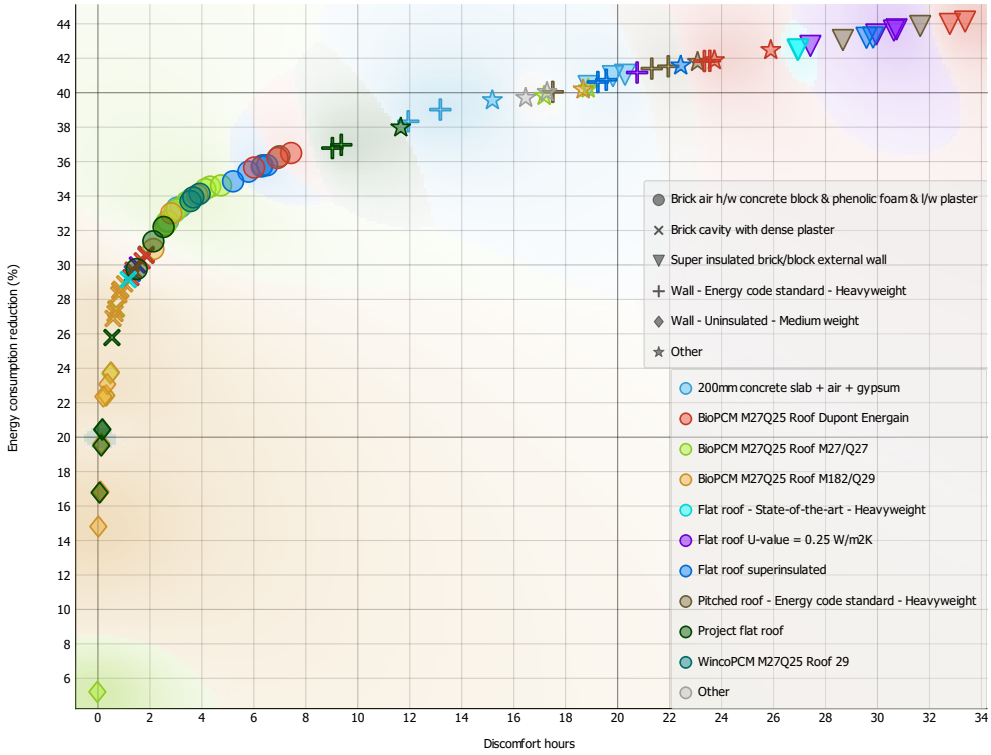

Figure 8. Results of energy consumption reduction (%) for cooling at Pareto's front for the H060.

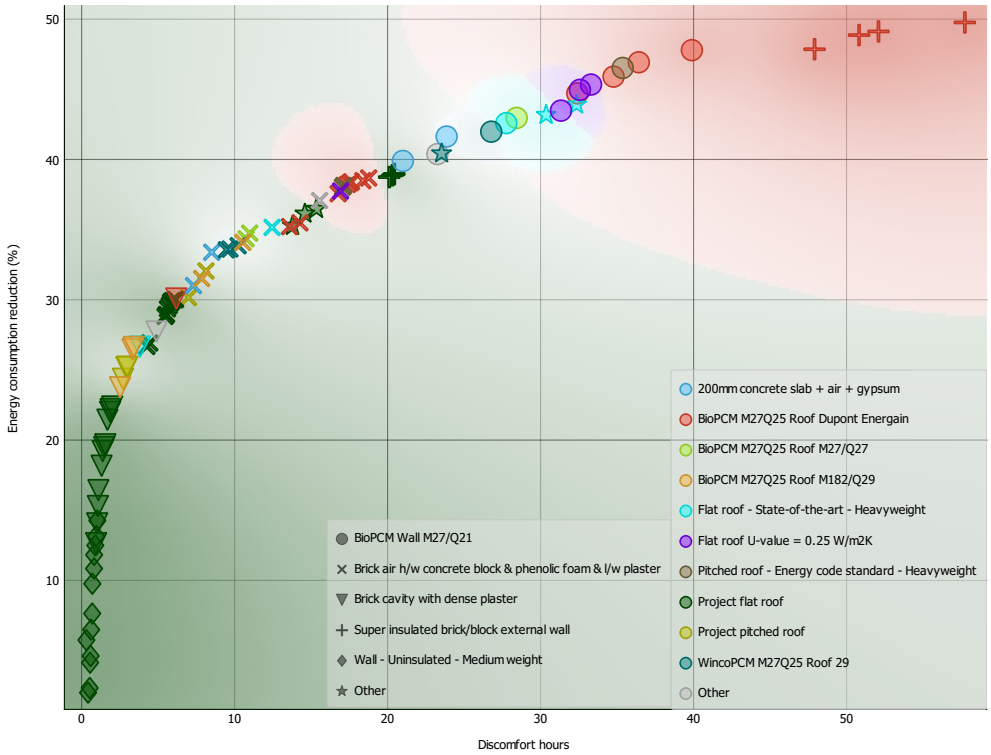

Figure 9. Results of energy consumption reduction (%) for cooling at Pareto's front for the H100.

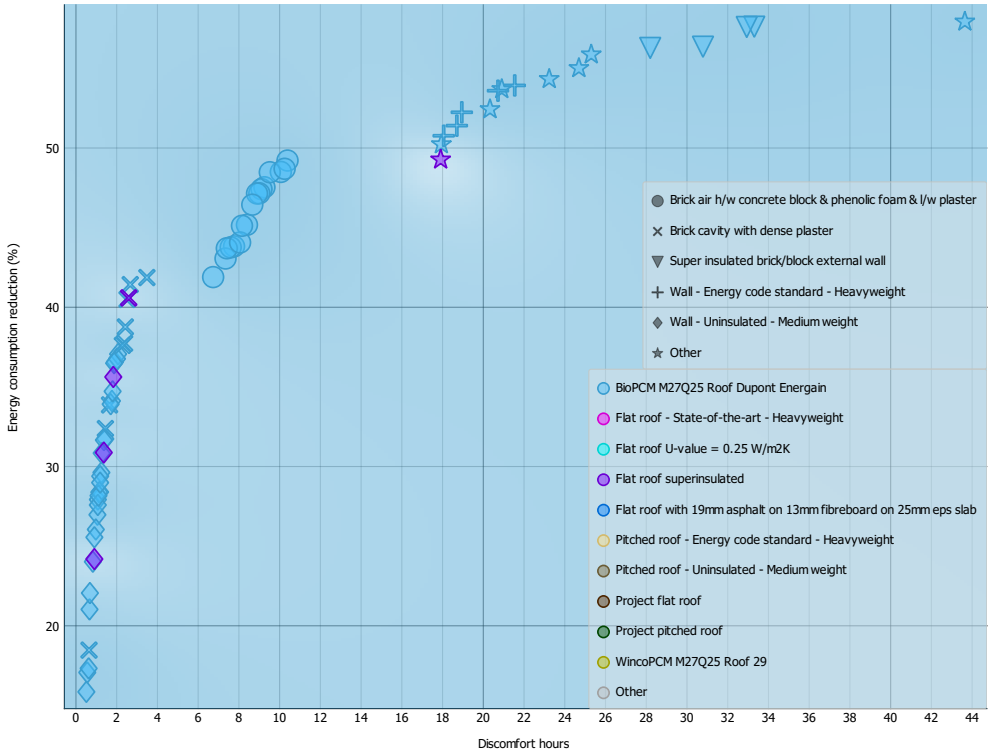

Figure 10. Results of energy consumption reduction (%) for cooling at Pareto's front for the H200.

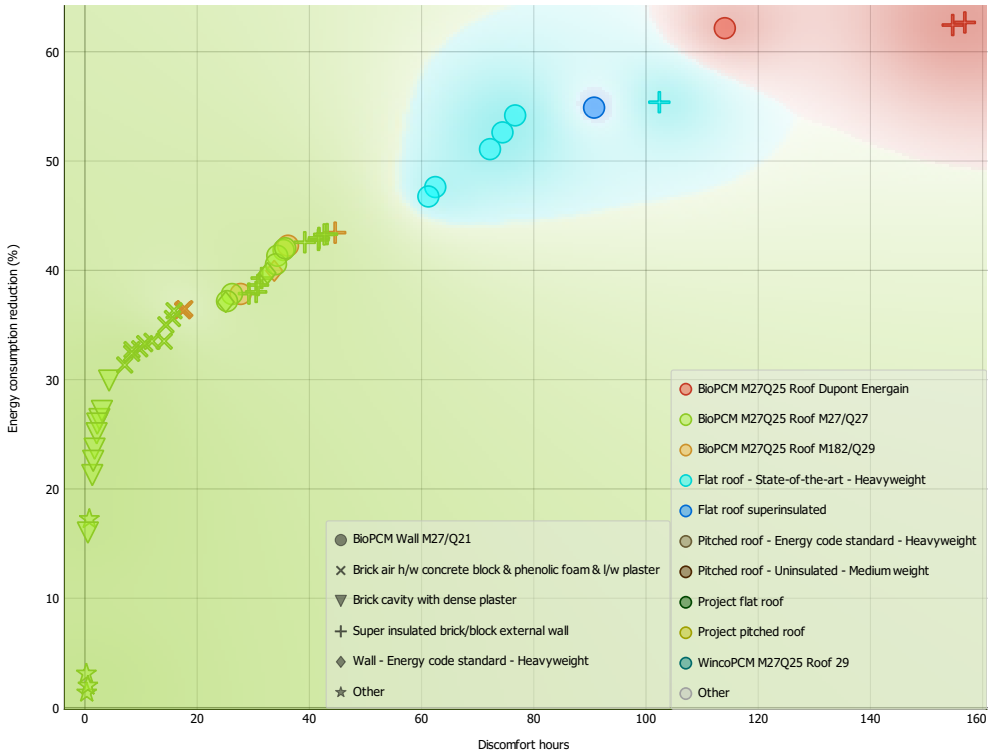

Figure 11. Results of energy consumption reduction (%) for cooling at Pareto's front for the OB.

3.3. Phase Change Behavior Analysis

As presented in the previous subsection, several options involving PCM in the envelope layouts were encountered at Pareto's front. To further assess this preference for choosing a PCM-based layout instead of a non-PCM-based layout, the most frequent envelope layout combination at Pareto's front (Section 3.1) was applied to each reference

building. The combination chosen for H060 is Rop13 + Wop6 + Gop4 + 250° + 30%WWR, for H200 is Rop12 + Wop5 + Gop4 + 220° + 30%WWR, and for OB is Rop12 + Wop5 + Gop4 + 220° + 30%WWR. Note here that the H100 was not considered for further study since a non-PCM-based layout was preferable.

This might help distinguish whether a PCM-based layout is preferred over a non-PCM-based layout because of their changes in physical properties at different solid/liquid phases or because of their very low values of thermal conductivity. To do this, the temperatures of both the external and internal surfaces of the buildings, as well as the average temperature, are evaluated to assess the phase state of the integrated PCM layer. Note here that, since phase change materials generally need a considerable amount of time exposed to higher (in the case of melting) or lower (in the case of solidification) temperatures to accomplish the phase change, this analysis also includes time periods.

In more detail, in the DesignBuilder's engine, EnergyPlus, a conduction finite difference solution algorithm has been incorporated for cases where the user needs to simulate phase change materials or variable thermal conductivity. The algorithm uses an implicit finite difference scheme coupled with an enthalpy-temperature function to account for phase change energy accurately (Equation (1)) [30].

$$c_p \rho \Delta x \frac{T_i^{j+1} - T_i^j}{\Delta t} = \frac{1}{2}\left(k_W \frac{T_{i+1}^{j+1} - T_i^{j+1}}{\Delta x} + k_E \frac{T_{i-1}^{j+1} - T_i^{j+1}}{\Delta x} + k_W \frac{T_{i+1}^{j} - T_i^{j}}{\Delta x} + k_E \frac{T_{i-1}^{j} - T_i^{j}}{\Delta x} \right) \quad (1)$$

where T refers to the nodes temperature, ρ is the material density, c_p is the specific heat capacity, and k_W and k_E correspond to the thermal conductivity for the interface between node i and node $i+1$, and for the interface between node i and node $i-1$, respectively. For the calculation, Δt is the chosen time step, Δx finite difference layer thickness (always less than construction layer thickness), i corresponds to the node being modeled, $i+1$ and $i-1$ refer to the node adjacent to the interior of the construction and the node adjacent to the exterior of the construction, respectively. Finally, $j+1$ and j represent the new time step and the previous time step, respectively. Equation (1) works together with the enthalpy and temperature relation: $h_i = HTF(T_i)$ where HTF is an enthalpy-temperature function that uses user input data [30].

- In the case of H060 + Rop13 + Wop6 + Gop4 + 250° + 30%WWR (Figure 12):

The PCM layer in Rop13 is located closer to the internal surface. As the Rop13 has a melting temperature point (MTP) of 29 °C, the complete phase change cycle is only achieved during the hottest month: from 9 March to 22 March. Among these days, the highest roof external surface temperature registered was between 54 and 59 °C on 18 March between 12h00 and 16h00. At night, the lowest temperature was around 21.5 °C at 6h00. The internal surface temperature varies between 33 and 35 °C between 12h00 and 16h00 on average. At night, the lowest temperature was around 32 °C at 6h00. For the external roof surface: the lowest temperature registered was about 21 °C on 9 March at 6h00, while the highest was about 45 °C at 12h00–17h00. For the internal roof surface: 28 °C on March 9th at 6h00, while the highest was about 32 °C at 12h00–17h00. During the coldest month, the hottest day registered was 10 November. For the highest roof, the external surface temperature registered was 50 °C at 13h00. At night, the lowest temperature was around 24 °C at 6h00. For the internal surface temperature, it was 27 °C between 12h00 and 16h00. At night, the lowest temperature was around 26.5 °C at 6h00. Finally, Figure 12a shows the envelope-surface averaged external vs. internal surface temperatures for the year simulation period. The temperature levels reached could translate into a suitable potential for Rop13 applications.

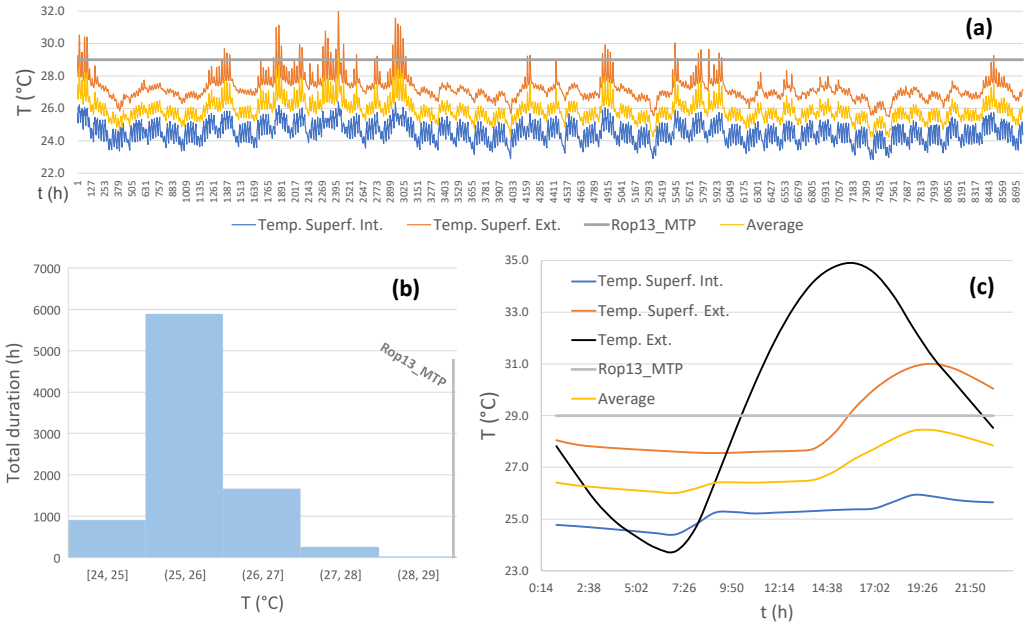

Figure 12. Local results from simulations for H060: (**a**) hourly temperatures for the entire year, (**b**) duration-based frequency for average temperature, and (**c**) hourly temperatures on 18 March.

- In the case of H200 + Rop12 + Wop5 + Gop4 + 220 ° + 30%WWR (Figure 13):

As the Rop12 has a melting temperature point (MTP) of 25 °C, by considering the average temperature (yellow line) the complete phase change cycle appears to never be achieved (Figure 13) since it never reaches values considerably lower than Rop12 MTP (gray line). Specifically, for the external roof surface, the higher temperature registered about 68 °C on 18 March between 12h00 and 15h00. On the same day, from 5h00 to 7h00, the external roof surface temperature was about 22 °C. At the internal roof surface, from 5h00 to 7h00, the temperature was about 30 °C, and 30 °C from 12h00 to 15h00. In addition, the internal roof surface temperature from 16h00 to 18h00 was about 32 °C.

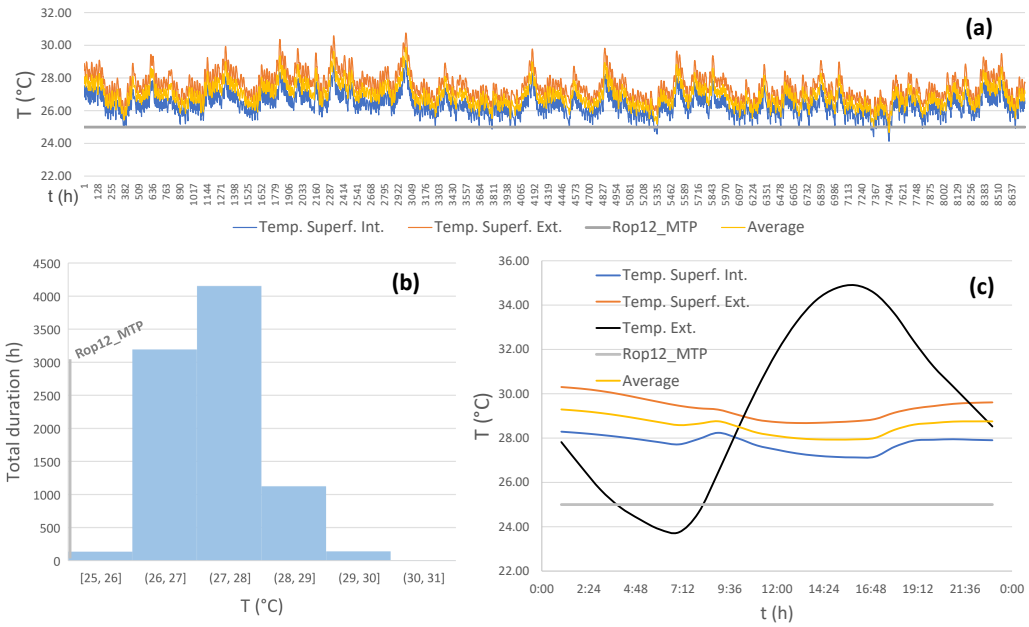

Figure 13. Local results from simulations for H200: (**a**) hourly temperatures for the entire year, (**b**) duration-based frequency for average temperature, and (**c**) hourly temperatures on 18 March.

- In the case of OB + Rop14 + Wop15 + Gop4 + 325° + 30%WWR (Figure 14):

As the Rop14 and Wop15 have a melting temperature point (MTP) of 27 °C and 21 °C, respectively, by considering the average temperature (light blue line) the complete phase change cycle appeared to be achieved only for the Rop14 (Figure 14a), since it reaches values considerably higher than and lower than Rop14 MTP (gray line). Specifically, for the external roof surface, the higher temperature reached registered about 58 °C on 18 March between 12h00 and 16h00. On the same day, from 3h00 to 7h00, the external roof surface temperature was about 22 °C. At the internal roof surface, from 3h00 to 7h00, the temperature was about 24 °C, and between 25 and 27 °C from 12h00 to 17h00. In the case of Wop15, Figure 14 shows that neither the internal nor the external surface reaches temperatures significantly lower than the Wop15 MTP, rendering its phase state a liquid state along the year.

The previous phase change behavior analysis indicates that a PCM-based layout with a PCM MTP of 27 °C is presumably the only material that would experience a complete phase change cycle in the case study. In addition, as shown in Figure 11, the implementation of Rop14 is preferable to lower the DH when combined with external-wall layouts other than Wop15, where a satisfactory compromise between low DH and high energy consumption reduction is met with walls including standard insulation degree. Similarly, the behavior encountered in Figures 13 and 14 indicates that a PCM with an MTP of 27 °C might also experience a complete phase change cycle.

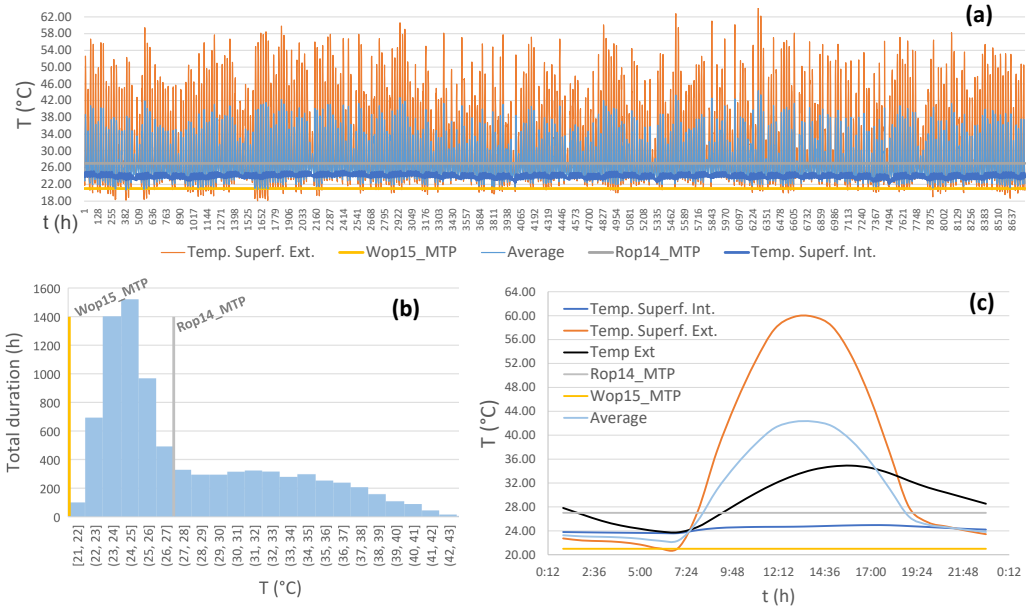

Figure 14. Local results from simulations for OB: (**a**) hourly temperatures for the entire year, (**b**) duration-based frequency for average temperature, and (**c**) hourly temperatures on 18 March.

4. Discussion

As shown in result analysis, the optimization procedure only provides feasible solutions among all the possible combinations. Several can be more frequent among these solutions according to the selected optimization criterion. Thus, those that repeat are much more likely to be the best options. Apart from this, the characteristics of the most feasible layouts can explain how the envelope should be structured to satisfy the desired thermal performance of a building. Hence, the results can be compared to other works with similar scopes according to the reachable optimization parameters. In this work, several PCM-related parameters are known: PCM layer thickness, PCM name, PCM layer location among envelope layers, envelope thickness, and thermal transmittance. Therefore, it is suggested to analyze the results taking into account PCM layout (related to location and

thickness) and PCM phase-changing operation (related to melting temperature and latent heat) of the optimum PCM-based envelope layouts (Rop12, Rop13, Rop14, and Wop15).

4.1. Statistical Focus

In the H060 building, Rop13 is the most frequent PCM-based solution found, followed by Rop15 and Rop12. PCM-based layouts for external walls did not satisfy the optimization criterion as well as non-PCM layouts. In the H100 building, PCM-based envelope layouts are not preferred, but still, the Rop12 and Wop15 appeared to be more than 14% and 17% as the optimum solution, respectively. In the H200 building, Rop12 is in over 92% of cases the best roof solution, but no PCM-based solution satisfied the optimization criterion for external walls. Finally, in OB, Rop14 is the most frequent optimum solution for roofs, while Wop15 is the most frequent option for external walls.

According to the optimization criterion, there is more possibility to reduce energy consumption by installing PCMs on roofs. Among the considered combinations, PCM-based roof configurations provide more optimum solutions than PCM-based wall configurations. This result fits the conclusions declared in Jia et al. [17], where it was shown that installing PCMs on roofs reduces energy consumption more than on walls but only focuses on net energy consumption. If implementation cost is considered, better reductions are found by means of installing PCMs on walls. Nonetheless, installing PCMs on both surfaces would permit even more energy savings.

4.2. PCM Layout

Among PCM-based optimum solutions, the selected ones for roof range from 0.124 m to 0.198 m, with a thermal transmittance from 0.991 W/m^2K to 0.113 W/m^2K. Moreover, the PCM thicknesses of Rop12, Rop13, and Rop14 are 148.4 mm, 74.2 mm, and 74.2 mm, respectively. The non-selected configuration, Rop15, has a thickness of 3 mm, but all the PCM-based configurations share the same surrounding layers. According to the optimization results across studied buildings, Rop12 appeared in Pareto's front at more than 30.1%, while Rop13 and Rop14 appeared at approximately 9% and 18%, respectively. Many authors [17,20,22,23,25] concluded that the thicker the PCM layer, the greater the energy consumption reduction. Since only Wop15 is obtained from the considered PCM-based wall configurations, there is no reason to compare it to other wall options. However, Wop15 is one of those with the largest PCM layer thicknesses, where from a total thickness of 270.1 mm, 148.4 mm are PCMs.

On the other hand, the PCM layer location in the envelope layout is frequently discussed. In this study, the configurations addressed contain PCM layers, which represent from 59.74% to 74.79% of the total thickness. Because of this, the PCM layer is distributed on both the outside and inside half of the wall envelope, having more options presented in the inner half. Neglecting volume distribution, the perimeter of the considered PCM layers is also nearer to the inside surface. This match was mentioned in Jia et al. [17], but it is contrary to the conclusions of other authors [18,20,25]. However, also in [18,20], it was established that PCM layer location has very little influence on energy savings, as long as the same PCM is considered. Nonetheless, in reviewed studies, the presence of the PCM layer in the envelope layout is much smaller than that considered in this study.

It is worth mentioning that all optimum envelope layouts had the same insulation layer. This is located before the PCM layer, as recommended by Imghoure et al. [25]. Therefore, the combinations in which inverting the order of the layers is considered did not match the suggested way of coupling insulation to PCM.

Finally, in PCM-based wall configurations, the same considerations about thickness, proximity to surfaces, and insulation layers are valid, although just one PCM-based configuration approved the optimization criterion.

4.3. Phase Changing Operation

The charge/discharge cycles are defined by melting temperature (°C), latent heat (kJ/kg), specific heat (kJ/kgK), energy storage capacity (kJ/m^2), and thermal conductivity (W/mK). Knowing the technical data of the selected PCM makes it possible to analyze the results. According to Jia et al. [17], the latent heat and energy storage capacity is one of the most important characteristics of achieving temperature fluctuation reductions beside climate zone. However, the PCMs of Rop12, Rop13, and Rop14 have the same latent heat and energy storage capacity.

The PCMs of Rop12 and Rop14 share the values of specific heat (2.5), thermal conductivity (0.15–0.25), and relative density (0.85–0.95 g/ml), while the PCM of Rop13 has 1.8, 10, and 1.47 times the values of specific heat, thermal conductivity, and relative density, correspondingly. However, since Rop12 is two times thicker than Rop13 and Rop14, the resultant thermal mass and energy storage capacity are bigger.

On the other hand, according to several authors [23–25], the melting temperature defines the effective operation of PCM since it restricts the thermal performance. For a complete charge/discharge cycle, the PCM must achieve the entire liquefaction and later a complete solidification. The melting temperature should be near the average temperature of the zone where the PCM layer is placed [25]. Thus, as seen in the result analysis by means of a histogram of temperature distribution, only Rop14 has a melting temperature (27 °C) which allows completing the cycle through the year. Nonetheless, despite an incomplete charge/discharge cycle, Rop12 and Rop13 were the most frequent optimum options at H060, H100, and H200. This suggests that PCM on liquid or solid phase provides better thermal performance than other considered combinations.

As seen, since the findings suggest similar inferences about using PCMs in tropical buildings compared to other authors' works, the results also showed that even in incomplete charge/discharge cycles, PCMs can still represent a better solution for building envelope enhancement. Therefore, the installation of PCM in tropical buildings can be completely acceptable depending on PCM type and envelope thermal behavior. Furthermore, using an approach based on the temperature of surfaces, it is possible to reduce computational cost and, consequently, speed up the selection of the most appropriate configurations.

5. Conclusions

The simulation study presented here evaluates various PCM-based envelope layouts in four case studies under the tropical climate of Panama City. Different criteria were used to determine an optimal PCM-based layout for such a climate through optimization analysis. In addition, several non-PCM-based layouts were included in this analysis to compare energy and thermal comfort performance. Among the considered combinations, PCM-based roof configurations provide more optimum solutions than PCM-based wall configurations. PCM layout with a melting temperature of 27 °C allowed completion of the PCM cycle throughout the year. Although other PCM layouts did not present a complete charge/discharge cycle, such as the most frequent options at H060, H100, and H200, it suggests that PCM on liquid or solid phase provides better thermal performance than other considered combinations. Thus, disregarding some technical differences among PCM types, PCM-based layers are more likely to be a better solution for tropical zones than conventional construction materials. However, the possibility of providing building thermal enhancement from PCMs considerably relies on envelope heat gain profiles. Furthermore, since average surface temperatures are used to estimate the PCM phase state, a numerical study based on discretization and average layer temperatures could verify these findings. However, this could lower the efficiency of audits and performance evaluation procedures to determine the technical feasibility of PCM layout implementation for large buildings.

Author Contributions: Original concept, supervision, and editing by M.C.A. and D.M.; introduction, figures and writing of most of the manuscript by M.C.A. and J.A. All authors have read and agreed to the published version of the manuscript.

Funding: This research was funded by Sistema Nacional de Investigación (SNI) as part of a Panamanian Institution Secretaria Nacional de Ciencia, Tecnología e Innovación (SENACYT, https://www.senacyt.gob.pa/, accessed on 26 March 2022) and the project code FID18-056.

Institutional Review Board Statement: Not applicable.

Informed Consent Statement: Not applicable.

Data Availability Statement: Not applicable.

Acknowledgments: The authors would like to thank the Research Group Energy and Comfort in Bioclimatic Buildings (ECEB, https://eceb.utp.ac.pa/, accessed on 26 March 2022) Faculty of Mechanical Engineering (https://fim.utp.ac.pa/, accessed on 26 March 2022) within the Universidad Tecnológica de Panamá (https://utp.ac.pa/, accessed on 26 March 2022) for their collaboration.

Conflicts of Interest: The funders had no role in the design of the study; in the collection, analyses, or—interpretation of data; in the writing of the manuscript, or—in the decision to publish the results.

References

1. International Renewable Energy Agency (IRENA). *Global Renewables Outlook: Energy Transformation 2050*; Technical Report; IRENA: Abu Dhabi, United Arab Emirates, 2020.
2. United Nations Environment Programme. *2021 Global Status Report for Buildings and Construction: Towards a Zero-Emission, Efficient and Resilient Buildings and Construction Sector*; Technical Report; United Nations: Nairobi, Kenya, 2021.
3. Cui, Q. Office Building Energy Saving Potential in Singapore. Master's Thesis, National University of Singapore, Singapore, 2006.
4. Fajilla, G.; Chen Austin, M.; Mora, D.; De Simone, M. Assessment of probabilistic models to estimate the occupancy state in office buildings using indoor parameters and user-related variables. *Energy Build.* **2021**, *246*, 15. [CrossRef]
5. Homod, R.Z.; Almusaed, A.; Almssad, A.; Jaafar, M.K.; Goodarzi, M.; Saharif, K.S. Effect of different building envelope materials on thermal comfort and air-conditioning energy savings: A case study in Basra city, Iraq. *J. Energy Storage* **2021**, *34*, 20. [CrossRef]
6. Araúz, J.; Mora, D.; Chen Austin, M. Assessment of Different Envelope Configurations via Optimization Analysis and Thermal Performance Indicators : A Case Study in a Tropical Climate. *Sustainability* **2022**, *13*, 20. [CrossRef]
7. Laaouatni, A.; Martaj, N.; Bennacer, R.; El Omari, M.; El Ganaoui, M. Phase change materials for improving the building thermal inertia. *Energy Procedia* **2017**, *139*, 744–749. [CrossRef]
8. Singh Rathore, P.K.; Shukla, S.K.; Gupta, N.K. Potential of microencapsulated PCM for energy savings in buildings: A critical review. *Sustain. Cities Soc.* **2020**, *53*, 101884. [CrossRef]
9. DesignBuilder Software Ltd. About DesignBuilder. 2022. Available online: https://DesignBuilder.co.uk/about-us (accessed on 7 June 2022).
10. Wu, S.; Yan, T.; Kuai, Z.; Pan, W. Thermal conductivity enhancement on phase change materials for thermal energy storage: A review. *Energy Storage Mater.* **2020**, *25*, 251–295. [CrossRef]
11. Rathore, P.K.S.; Shukla, S.K. An experimental evaluation of thermal behavior of the building envelope using macroencapsulated PCM for energy savings. *Renew. Energy* **2020**, *149*, 1300–1313. [CrossRef]
12. Hakim, I.I.; Putra, N.; Agustin, P.D. Measurement of PCM-concrete composites thermal properties for energy conservation in building material. *AIP Conf. Proc.* **2020**, *2255*, 0300661–0300667. [CrossRef]
13. Cárdenas-Ramírez, C.; Gómez, M.A.; Jaramillo, F.; Cardona, A.F.; Fernández, A.G.; Cabeza, L.F. Experimental steady-state and transient thermal performance of materials for thermal energy storage in building applications: From powder SS-PCMs to SS-PCM-based acrylic plaster. *Energy* **2022**, *250*, 123768. [CrossRef]
14. Rathore, P.K.S.; Shukla, S.K. Enhanced thermophysical properties of organic PCM through shape stabilization for thermal energy storage in buildings: A state of the art review. *Energy Build.* **2021**, *236*, 110799. [CrossRef]
15. U.S Department of Energy's Building Techologies Office. *EnergyPlus 9.6.0*; U.S Department of Energy's Building Techologies Office: Washington, DC, USA, 2021.
16. Sarri, A.; Bechki, D.; Bouguettaia, H.; Al-saadi, S.N. Effect of using PCMs and shading devices on the thermal performance of buildings in different Algerian climates . A simulation-based optimization. *Sol. Energy* **2021**, *217*, 375–389. [CrossRef]
17. Jia, J.; Liu, B.; Ma, L.; Wang, H.; Li, D.; Wang, Y. Case Studies in Thermal Engineering Energy saving performance optimization and regional adaptability of prefabricated buildings with PCM in different climates. *Case Stud. Therm. Eng.* **2021**, *26*, 101164. [CrossRef]
18. Sangwan, P.; Mehdizadeh-rad, H.; Wai, A.; Ng, M.; Atiq, M.; Rehman, U.; Nnachi, R.C. Performance Evaluation of Phase Change Materials to Reduce the Cooling Load of Buildings in a Tropical Climate. *Renew. Energy* **2022**, *148*, 402–416. [CrossRef]
19. Kameni, M.; Christophe, J.; Noelson, V.; Saadi, I.; Kenfack, H.; Andrianaharinjaka, A.z.F.R.; Foumouo, D.; Barahimo, J.; Reiter, S. Application of phase change materials , thermal insulation , and external shading for thermal comfort improvement and cooling energy demand reduction in an o ffi ce building under di ff erent coastal tropical climates. *Sol. Energy* **2020**, *207*, 458–470. [CrossRef]

20. Bimaganbetova, M.; Memon, S.A.; Sheriyev, A. Performance evaluation of phase change materials suitable for cities representing the whole tropical savanna climate region. *Renew. Energy* **2020**, *148*, 402–416. [CrossRef]
21. Berrocal, D.; Aranda, R.; Santamaría, S.; Vigil, A.; Chen Austin, M. El cambio de fase como estrategia pasiva: Evaluación del rendimiento térmico-energético en edificaciones en Panamá. *I+D Tecnológico* **2022**, *177*, 12. [CrossRef]
22. Saxena, R.; Rakshit, D.; Kaushik, S.C. Experimental assessment of Phase Change Material (PCM) embedded bricks for passive conditioning in buildings. *Renew. Energy* **2020**, *149*, 587–599. [CrossRef]
23. Yu, J.; Yang, Q.; Ye, H.; Luo, Y.; Huang, J. Thermal performance evaluation and optimal design of building roof with outer-layer shape-stabilized PCM. *Renew. Energy* **2020**, *145*, 2538–2549. [CrossRef]
24. Bhamare, D.K.; Rathod, M.K.; Banerjee, J. Numerical model for evaluating thermal performance of residential building roof integrated with inclined phase change material (PCM) layer. *J. Build. Eng.* **2020**, *28*, 101018. [CrossRef]
25. Imghoure, O.; Belouaggadia, N.; Ezzine, M.; Lbibb, R.; Younsi, Z. Performance evaluation of phase change materials for thermal comfort in a hot climate region. *Appl. Therm. Eng.* **2021**, *186*, 116509. [CrossRef]
26. Kottek, M.; Grieser, J.; Beck, C.; Rudolf, B.; Rubel, F. World Map of the Köppen-Geiger climate classification updated. *Meteorol. Zeitschrif* **2006**, *15*, 259–263. [CrossRef]
27. Hasan, M.; Alam, S.; Ahmed, D.H. Effect of phase change material on the heat transfer rate of different building materials. *AIP Conf. Proc.* **2017**, *1919*, 20029. [CrossRef]
28. De León, L.; Student, E.; Cedeño, M.; Mora, D.; Chen Austin, M. Towards a Definition for Zero Energy Districts in Panama: A Numerical Assessment of Passive and Active Strategies. In Proceedings of the 9th LACCEI International Multi-Conference for Engineering, Education, and Technology: "Prospective and trends in technology and skills for sustainable social development", "Leveraging emerging technologies to construct the future", Virtual Edition, 9–10 December 2021. [CrossRef]
29. Zhang, Y.; Jankovic, L. JEA, An Interactive Optimisation Engine for Building Energy Performance Simulation. In Proceedings of the 15th IBPSA Conference, San Francisco, CA, USA, 7–9 August 2017; p. 2232. [CrossRef]
30. U.S. Deparment of Energy. EnergyPlus-Engineering Reference. Available online: https://doi.org/https://energyplus.net/assets/nrel_custom/pdfs/pdfs_v22.1.0/EngineeringReference.pdf (accessed on 20 June 2022).